

Use Golden Section Method to Fit Involute Curve of Scroll Compressor

Chunqi Tang*, Fugui Yuan

University of Shanghai for Science and Technology, Shanghai, China

*Tangchunqi2022@foxmail.com

Abstract

Based on multiple experiments using involute fitting programs, it was found that the deviation decreases initially as the computed radius approaches the actual base circle radius, then increases, exhibiting a minimum value. Therefore, a method based on the golden section method is proposed, requiring minimal computation to identify the optimal base circle radius corresponding to the minimum deviation.

Keywords

Scroll Compressor; Base Circle; Involute Fitting; Golden Section Method; Profile.

1. Introduction

With the expanding scope of engineering applications, there are increasing demands for the machining accuracy of spiral contours[1]. The accuracy directly impacts the precision and stability of transmission movements and the uniformity of load distribution. Higher profile accuracy leads to improved transmission movement precision, mechanical efficiency, load-bearing capacity, wear resistance, fatigue life, and reduced mechanical vibration and noise.

Traditional machining methods often fail to meet modern requirements for high precision, flexibility, and efficiency in processing complex surfaces. As a result, multi-axis universal CNC machining has become a significant research focus. The surface smoothness and complexity of digital models used in machining are critical factors affecting final machining quality[4], making accurate mathematical modeling based on known measurement points highly meaningful.

Currently, contour types include circular involute, circular arc, and higher-order curves. Analysis of each contour feature indicates that circular involutes offer stable performance and are easy to process[3]. Jianguo Qiang suggests that the impeller profile of the scroll compressor ideally follows the base circle involute due to its low sensitivity to errors and more stable dynamic characteristics[2]. Therefore, this study focuses on fitting the circular involute.

In contrast to purely theoretical fitting methods, the fitting approach in this paper is grounded on real impeller data. The measured data consist of a series of two-dimensional coordinate points that are non-eccentric to the origin and typically follow the distribution of an involute rotating counterclockwise from inside to outside. The involute usually spans more than one complete turn.

Furthermore, the paper analyzes the interplay between measurement accuracy, fitting precision, and fitting effectiveness. It demonstrates robust fitting capabilities even when measurement errors are significant. Compared to hypothetical point replacement methods, this approach significantly reduces computational complexity and does not necessitate extensive measurement times.

2. Mathematical Description of the Fitting Problem

2.1. General Fitting Method

Yang Yexi proposed a model similar to gear fitting. Based on the principle of least squares and minimizing the sum of squared deviations between measured points and assumed fitting points, a model was established to determine the center coordinates of the base circle and the starting angle of the involute on a standard involute template [5]. Following Yang Yexi's concept, the fitting approximations under different assumed radii are scientifically described, rather than judged subjectively based on visual inspection. As shown in the figure below, the sum of squared deviations between the measurement points and assumed fitting points in Figure A is greater than that in Figure B. Therefore, the fitting effect of Figure B is good, and the assumed radius corresponding to Figure B is closer to the true value.

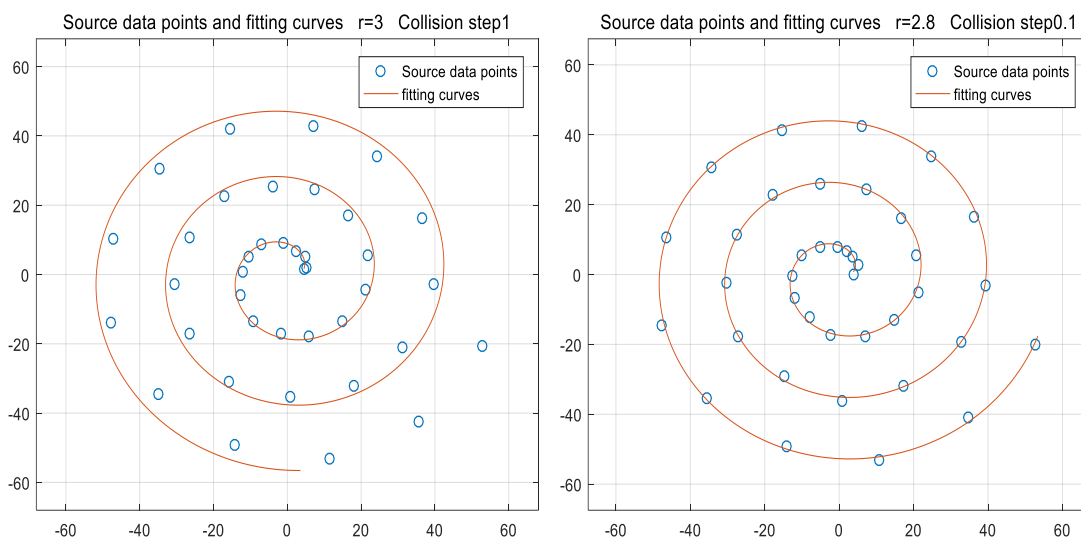


Fig. 1 Comparison of different fitting effects

From the diagram, it can also be observed that the plot of the involute differs from typical function graphs in the coordinate system. Vertical lines perpendicular to the x-axis can intersect the involute at multiple points, making polynomial fitting unsuitable for fitting the entire curve. However, it is impractical to solve the equation using the coordinates of a single point in Cartesian coordinates, as there would be infinitely many solutions, and it is impossible to determine a unique corresponding development angle and base circle radius.

Involute equation:

$$X = R * (\cos(\varphi A) + \varphi * \sin(\varphi));$$

$$Y = R * (\sin(\varphi A) - \varphi * \cos(\varphi));$$

2.2. Definition of Deviation

I Furthermore, due to inherent measurement errors that deviate from true values, substituting a single measurement point into the equation to derive its unique development angle and base circle radius is impossible. Consequently, generating a fitting point based on the measurement point and assumed radius becomes unfeasible, preventing the calculation of the deviation between the measurement point and the fitting point. This necessitates a reconsideration of how deviations are calculated.

To address the deviation between the nth measurement point and the nth fitting curve, this study employs the MD method (finding the difference between each measuring point and all

fitting points sequentially, and recording the minimum deviation as the deviation between the measuring point and the fitting curve). For example, if the measuring point is [1, 1], and the fitting points under the assumed radius are [0.9, 0.9], [0.8, 0.8], [1.1, 1.0], [1.3, 1.2], the differences yield distance deviations of [0.1414, 0.2828, 0.1000, 0.3606]. According to the deviation definition, 0.1000 represents the fitting deviation of this measuring point.

Similarly, applying the MD method to N measuring points yields N deviations. Squaring each deviation and then averaging them provides the average deviation between the fitting curve and the measured value under the assumed radius.

2.3. Unexpected Discovery

Through multiple fitting attempts, as depicted in the following figure, it was observed that the x-axis represents the assumed radius. By continuously computing the deviation generated by this radius at each coordinate, the y-axis represents the corresponding average deviation. It was discovered that there exists a minimum value when the collision radius falls between 0 and 10, which represents the final fitting radius. Near this minimum point, there are also two additional minimum points (r=1.8, r=4.4). Furthermore, it was noted that there is a singular valley near the final fitting radius (approximately 2.5-3.5). The challenge lies in automatically defining this neighborhood within the program and leveraging the golden section method to significantly streamline the computation process.

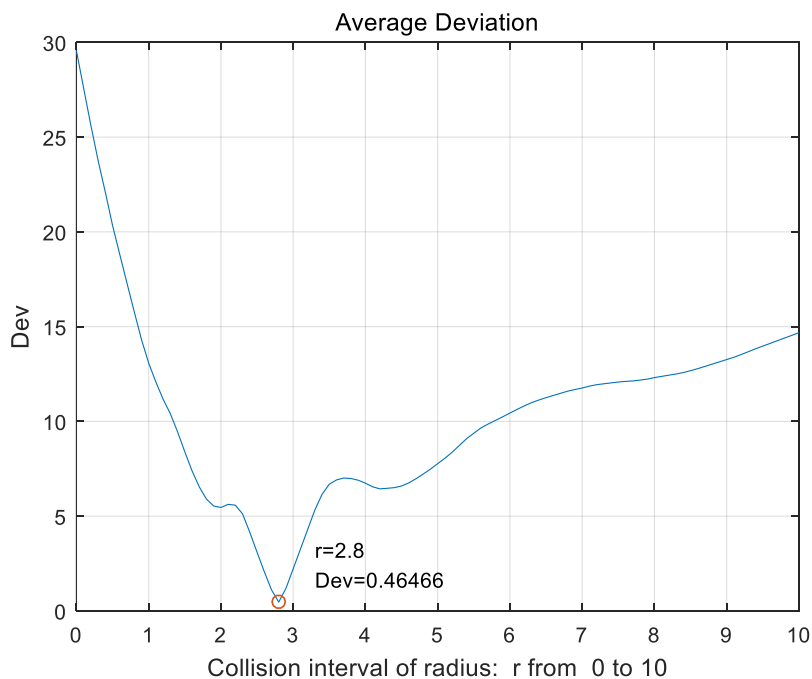


Fig. 2 Average Deviation

When fitting involute curves, it is feasible to compute using numerous assumed values colliding with measurement points. Simply calculate their deviations based on the given assumed radius, then select the radius corresponding to the minimum deviation as the final fitting radius. For tens of thousands of assumed points, computers can tolerate computation based on the aforementioned method. However, higher precision may necessitate millions of points, making computations time-consuming and cumbersome. Another method to select the optimal fitting radius is using the golden section method described in this paper. Prior to use, one must address issues related to partitioning boundaries due to multiple valleys and how to apply the golden section method. In analyzing the geometric characteristics of involute curves, a method

was found to characterize the neighborhood. As shown in the figure below, according to the principles of involute curves, let A be a point on the involute curve, let line AB be the generatrix passing through point A, intersection B of the next circle and circle O, let line OA intersect with the original point O, and point C of the next circle extend in the opposite direction, angles φ_A , φ_B , and φ_C are the expansion angles of each point (expansion angle is not polar angle), " α_A " and " ρ_A " are the polar angle and polar radius of point A on the polar axis, and r is the radius of the basic circle, so there are coordinates:

$$X_A = R * (\cos(\varphi_A) + \varphi_A * \sin(\varphi_A));$$

$$Y_A = R * (\sin(\varphi_A) - \varphi_A * \cos(\varphi_A));$$

$$X_B = R * (\cos(\varphi_B) + \varphi_B * \sin(\varphi_B));$$

$$Y_B = R * (\sin(\varphi_B) - \varphi_B * \cos(\varphi_B));$$

$$X_C = R * (\cos(\varphi_C) + \varphi_C * \sin(\varphi_C));$$

$$Y_C = R * (\sin(\varphi_C) - \varphi_C * \cos(\varphi_C));$$

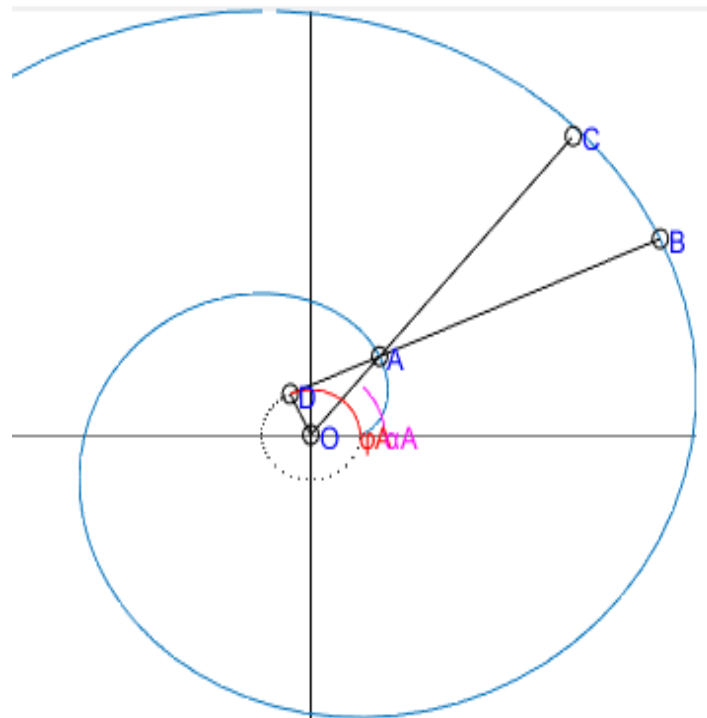


Fig. 3 Involute geometry

When the intervals between collection points are small, $|AC| \approx |AB| = 2\pi R$. Using this formula to estimate the radius of the base circle is a good choice. Let $\Delta\rho = |AC| = |\rho_A - \rho_C| = 2\pi R\rho$, where $R\rho$ is the radius of the base circle obtained using the estimation method. Hence, $R\rho = \Delta\rho / 2\pi$ allows us to determine the estimated radius of the base circle.

In practical scenarios, our human eyes can distinguish certain measurement points A and C well because the brain compensates for missing points. We can clearly know which circle a point belongs to and whether there is a corresponding point in the next circle. However, computers cannot directly distinguish whether these measurement points are "A" or "C". Therefore, we need algorithms to partition the data into quadrants, extract valid points, and then perform calculations. As shown in the figure below, the "O" in the diagram represents that a measurement point can find a valid "C" point in the next circle, and $R\rho$ can be calculated. The "x" point indicates that no valid "C" point can be found at this point.

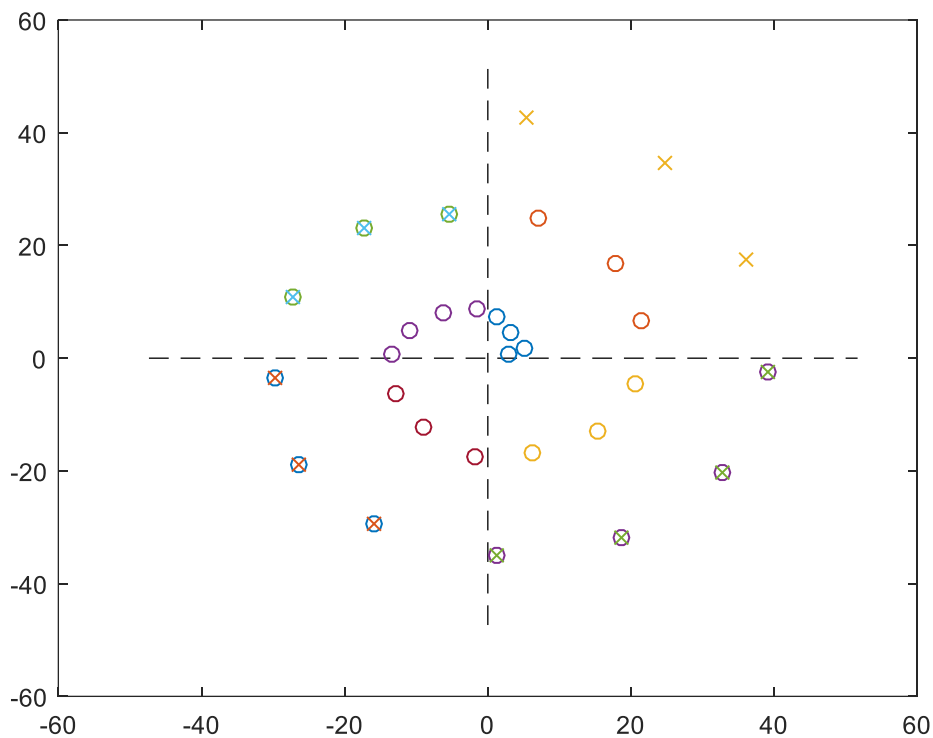


Fig. 4 Processing diagram of measuring points

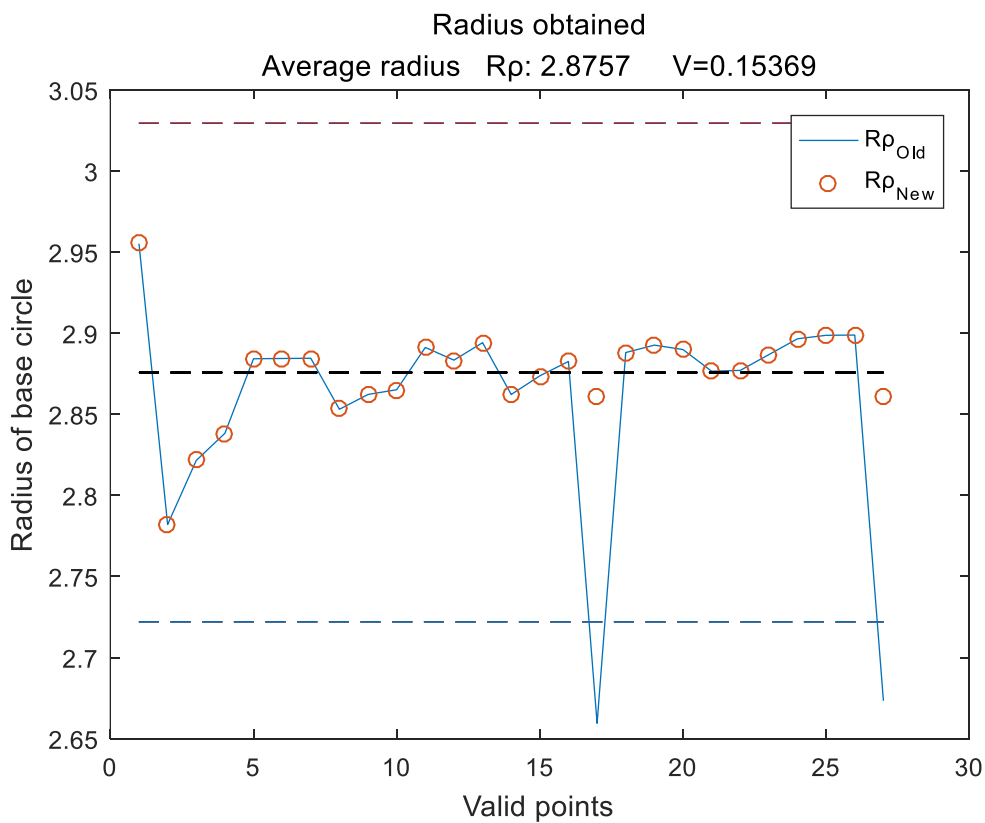


Fig. 5 Arrangement of average error

In the program, calculate all effective points and then compute the rough radius R_p , with sorting results shown in the diagram below. The ordinate represents the serial number of effective points, not the sequence number of measurement data. Select points calculable from the measurement data and record them as effective points. The ordinate corresponds to the calculated rough radius of the measuring point relative to its effective serial number, where R_p is summarized with the measurement point serial number depicted in solid blue lines. Additionally, due to the randomness of measurements, calculating the rough radius can lead to gross errors, where the rough radius significantly exceeds the average distribution. Therefore, it is necessary to exclude corresponding gross errors, taking the average R_p as the final neighborhood center, with a neighborhood radius of V , where $V=S*t$, S being the variance of deviations and $t=3$. As shown in the figure below, calculate R_p with the serial number of effective points as the horizontal axis and its value as the vertical axis. The middle dashed line in the graph represents the average R_p , while the upper and lower dashed lines indicate $R_p \pm V$, treating exceeding values as gross errors. Furthermore, the distribution of R_p exhibits periodicity, likely due to the effective point serial numbers being discussed based on quadrant grouping, causing fluctuations in periodic lines.

2.4. The Application of the Golden Section Method.

After conducting numerous experiments, it was observed that within the established neighborhood interval, graphs depicting average deviation and assumed radius generally exhibit a single-valley characteristic. Only a few regions on the edges show an additional downward trend, meeting the criteria for the golden section method, as shown in the following figure. Additionally, data processed under various measurement errors consistently indicate that the valley tends to slope leftward, potentially exceeding the neighborhood boundaries. Specific reasons for this behavior are not discussed here. To prevent the actual radius from exceeding the neighborhood interval, adjustments can be made to the neighborhood center. Based on extensive experimentation, the neighborhood interval is shifted leftward by $k * V$, with a correction coefficient of $k=0.2$.

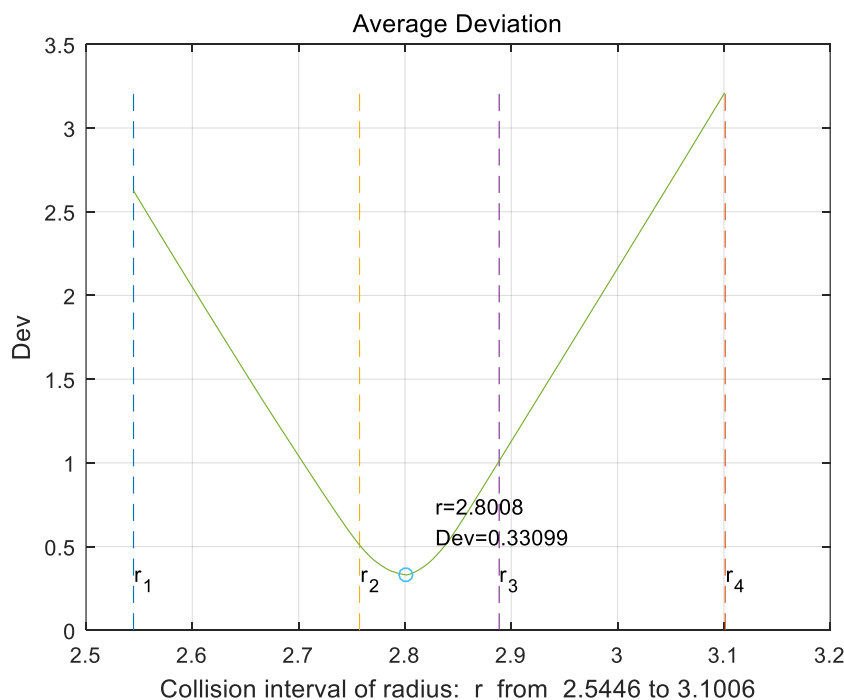


Fig. 6 Use the golden section method in the neighborhood

If the initial neighborhood interval is $[r1, r4]$, applying the golden section method gives us $r2 = r4 - 0.618 * (r4 - r1)$ and $r3 = r1 + 0.618 * (r4 - r1)$. Here, $r2$ is chosen as the final output value. During the first iteration, it is observed that the average deviation $Dev2$ corresponding to $r2$ is lower than the average deviation $Dev3$ of $r3$. This indicates that the minimum point must lie within $[r1, r3]$. Therefore, the neighborhood interval for the next iteration is adjusted to $[r1, r3]$, and $r2$ is recorded at this point. In subsequent iterations, if the difference between the old $r2$ and the new $r2$ falls below an allowable threshold, the loop terminates. The new $r2$ and $Dev2$ are then outputted as the fitting deviation and the radius of the base circle, representing the final fitted values.

3. Application and Discussion

After configuring the measurement error, the program was executed, and the results are depicted in the following figure. Upon comparing the measured data with the fitted curve, it was observed that the average deviation is less than half of the measured deviation, indicating a good fit.

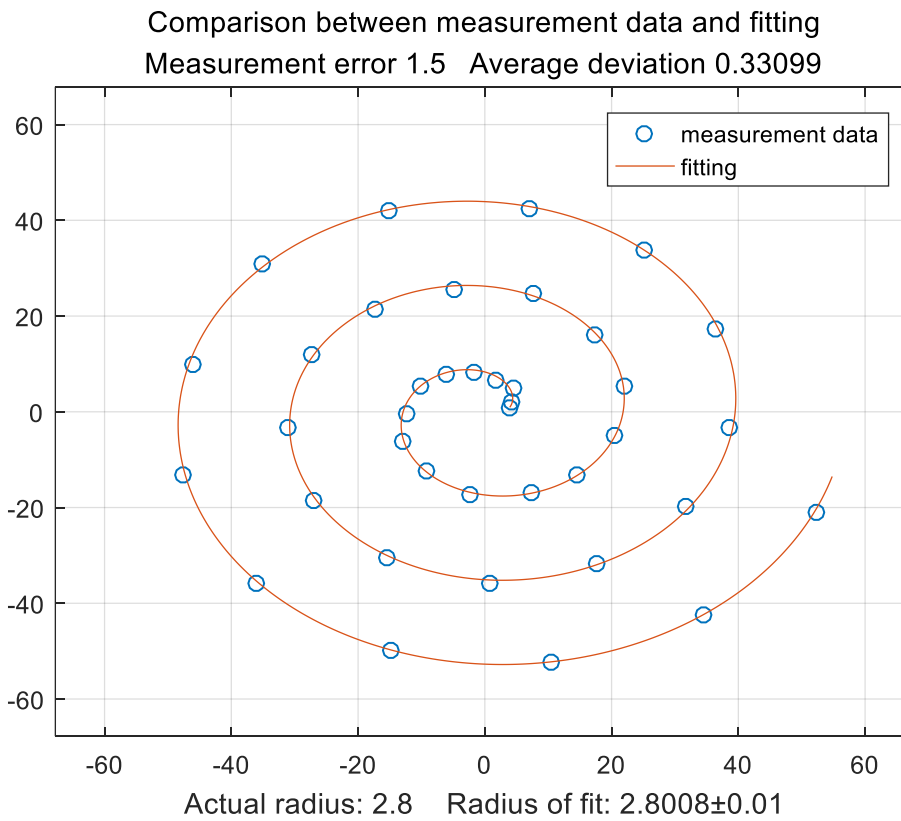


Fig. 7 Comparison between measured data and fitted curve

This paper explores the "influence of fitting accuracy on fitting effect". Using a fitting accuracy $FitAc=0.005$ as an example, the accompanying figure illustrates the relationship. The x-axis represents the measurement error associated with the measuring instrument, typically less than 0.1 cm. The y-axis denotes the final fitting deviation Dev corresponding to each measurement error. In the figure, a horizontal dashed line indicates the fitting accuracy threshold, representing the maximum permissible deviation under $FitAc$. Generally, as the measurement error decreases, the deviation Dev approaches this horizontal line more closely. An oblique line serves as an effective fitting boundary, exhibiting a positive proportional relationship with a slope of 1. The region below this boundary line indicates effective fitting,

where Dev changes notably with varying measurement errors, demonstrating strong fitting effectiveness. Conversely, above the boundary line, Dev decreases more gradually with decreasing error.

In practical terms, for a FitAc of 0.005, the recommended actual measurement error is 0.06 cm. The figure suggests that exceeding this recommended error leads to larger deviations Dev, which is detrimental to fitting accuracy. Opting for a lower measurement error (using a higher precision instrument) results in a slower decrease in Dev, indicating increased measurement costs without proportionate improvements in fitting accuracy. Furthermore, while higher fitting accuracy may enhance fitting effectiveness, it can also lead to increased computational costs. Thus, there is a trade-off between achieving higher fitting accuracy and managing computational resources effectively.

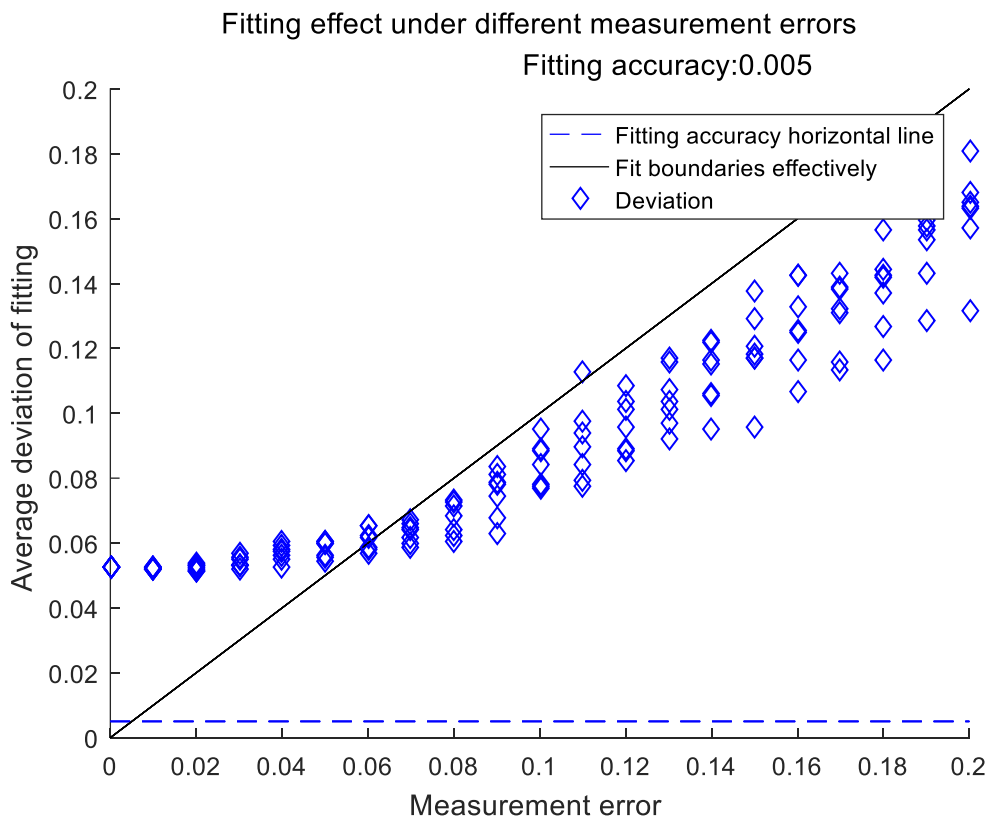


Fig. 8 Fitting effect under different measurement errors

4. Conclusion

Based on the comprehensive application of the golden section method in fitting involutes, it efficiently determines the base circle radius with minimal deviation. Analysis of deviations from various hypothetical points confirms convergence near the true radius, satisfying the precondition for employing the golden section method.

Furthermore, through geometric analysis of involutes, a method is derived for estimating the base circle radius. This method offers a numerical foundation for narrowing the analysis interval automatically within the golden section method by computer.

Additionally, the paper explores the impact of fitting accuracy on fitting effectiveness. It concludes that selecting an appropriate fitting accuracy based on measurement error can mitigate computational overhead.

References

- [1] AHMAD M, MARJAN M, TRACIE B. Compression chamber volume analysis for corotating scroll compressors [J]. International Journal of Refrigeration, 2020, 112: 172-188.
- [2] Jianguo Qiang, Zhenquan Liu, Scroll profiles in scroll compressors: General criteria and error sensitivity, International Journal of Refrigeration, Volume 36, Issue 7, 2013.
- [3] Ming Ling, Siying Ling, Xiangsheng Liu, Zhaoyao Shi, Liding Wang. Determination method of unwrapped length in involute pure rolling measurement [J]. Chinese Journal of Scientific Instrument, 2022, 43(08): 101-108. DOI: 10.19650/j.cnki.cjsi.J2209800.
- [4] Jin Xie, Mingshan Zou, Xiaoling Cui. Influence of curvature distribution characteristics of complex freeform surfaces on CNC milling performance [J]. Journal of Mechanical Engineering, 2009, 45(11): 158-162.
- [5] Yeqian Yang. Influence of coordinate system establishment errors on measurement results of off-axis gear measuring machines and their reduction [D]. Xi'an Technological University, 2022. DOI: 10.27391/d.cnki.gxagu.2022.000346.

Appendix A. Fitting effect under different measurement errors

```

%% Set parameters
phi=1: 0.5: 20;
r0=2.8;
X=r0.*(cos(phi)+phi.*sin(phi));
Y=r0.*(sin(phi)-phi.*cos(phi));
[~,nX]=size(X);
h_A=0.01;%Angle accuracy
MaxMeasurementError=0.2; %Maximum measurement error
FitAc=0.005; %Fitting precision FitAc
num=20;
%% calculation
MErr=0: MaxMeasurementError/num: MaxMeasurementError;
DEV= ;
for err=MErr
    X=X+err*(rand(1,nX)-0.5); Y=Y+err*(rand(1,nX)-0.5); %Artificial error
    Phi=0: h_A: 30; %Developed angle matrix constructed
    r1=2.5; r4=3.3; r2=2.5; ERR=FitAc+1;
    while ERR>FitAc %Calculate the radius and its deviation
        r2_=r2; r2=r4-0.618*(r4-r1); r3=r1+0.618*(r4-r1);
        X2=r2.*(cos(Phi)+Phi.*sin(Phi)); Y2=r2.*(sin(Phi)-Phi.*cos(Phi));
        X3=r3.*(cos(Phi)+Phi.*sin(Phi)); Y3=r3.*(sin(Phi)-Phi.*cos(Phi));
        XX2= ; YY2= ; XX3= ; YY3= ;
        for i=1:nX
            [~, n]=min((X2-X(i)).^2+ (Y2-Y(i)).^2); XX2(end+1)=X2(n); YY2(end+1)=Y2(n);
            [~, n]=min((X3-X(i)).^2+ (Y3-Y(i)).^2); XX3(end+1)=X3(n); YY3(end+1)=Y3(n);
        end
        Dev2=sum(sqrt( (XX2-X).^2+ (YY2-Y).^2))/nX;
        Dev3=sum(sqrt( (XX3-X).^2+ (YY3-Y).^2))/nX;
        if Dev2< Dev3; r4=r3; else r1=r2; end
        r_mean=(r1+r4)/2; ERR=abs(r2-r2_);
    end

    DEV(end+1)=Dev2;
end

%% figure
hold on, plot(MErr,MErr*0+FitAc,'--b')
hold on, plot(MErr,MErr,'k')
hold on, plot(MErr,DEV,'db')
title({'Fitting effect under different measurement errors'};...
    [' Fitting accuracy:',num2str(FitAc)])
legend('Fitting accuracy horizontal line','Fit boundaries effectively','Deviation')
xlabel(['Measurement error '])

```

ylabel(['Average deviation of fitting '])